




Assessing the effectiveness of landslide slope stability by analysing structural mitigation measures and community risk perception

A. S. M. Maksud Kamal¹ · Farhad Hossain² · Bayes Ahmed³  · Md. Zillur Rahman¹ · Peter Sammonds³

Received: 9 December 2022 / Accepted: 24 March 2023 / Published online: 18 April 2023
© The Author(s) 2023

Abstract

Rainfall-induced landslides seriously threaten hilly environments, leading local authorities to implement various mitigation measures to decrease disaster risk. However, there is a significant gap in the current literature regarding evaluating their effectiveness and the associated community risk perception. To address this gap, we used an interdisciplinary and innovative approach to analyse the slope stability of landslides, evaluate the effectiveness of existing structural mitigation measures, and assess the risk perception of those living in danger zones. Our case study focused on the Kutupalong Rohingya Camp (KRC) in Cox's Bazar, Bangladesh, which is home to over one million Rohingya refugees from Myanmar. Although various structural and non-structural countermeasures were implemented in the KRC to mitigate the impact of landslides, many of them failed to prevent landslides from occurring. We utilised a variety of methods from the physical sciences, including the infinite slope, limit equilibrium (LEM), and finite element (FEM) approaches, to calculate the factor of safety (FoS) for specific slopes. Additionally, in the social sciences domain, we conducted a questionnaire survey of approximately 400 Rohingya participants to assess the community's perception of the interventions and the degree of disaster risk. Our findings indicated that slopes with a gradient greater than 40° were unstable ($\text{FoS} < 1$), which was present throughout the entire KRC area. The effectiveness of the LEM and FEM methods was evaluated for four dominant slope angles (40° , 45° , 50° , and 55°) under varying loads (0, 50, and 100 kN/m^2). The slopes were found to be stable for lower slope angles but unstable for higher slope angles ($> 50^\circ$) and increased overburden loads ($50\text{--}100 \text{ kN/m}^2$). Different mitigation measures were tested on the identified unstable slopes to assess their effectiveness, but the results showed that the countermeasures only provided marginal protection against landslides. Survey results revealed that at least 70% of respondents believed that concrete retaining walls are more effective in reducing landslide occurrence compared to other measures. Additionally, about 60% of the respondents questioned the reliability of the existing structural mitigation measures. The study also found that the cohesion and friction angle of lower sandstone and the cohesion of upper soil layers are important factors to consider when designing and implementing slope protection countermeasures in the KRC area.

Keywords Landslides · Slope stability · Countermeasure · Disaster risk perception · Structural mitigation measures

1 Introduction

Landslides frequently occur in the tropical and sub-tropical regions where intense monsoon and elevated terrains accompanied by thick alluvial, colluvial, and residual soil covers are observed (Garland and Olivier 1993; Larsen and Torres-Sánchez 1998; Hungr et al. 2014; Zhuang et al. 2018). It is a common geological phenomenon frequently occurring in hilly/mountainous areas and causes severe life and property losses (Kjekstad and Highland 2009; Petley 2012; Froude and Petley 2018). Using countermeasures' rational design is necessary to protect people and infrastructure at risk. The mechanisms causing the failure of slopes and logical analysis of slope stability to select proper countermeasures are urgent topics of interest for research. The performance evaluation of the chosen landslide countermeasures is crucial to improve the disaster resilience of the people at risk of slope failure. The perception of the local community on the implemented landslide mitigation measure is also essential for disaster risk reduction (DRR).

The studies of the landslide mechanisms and behaviours of slope materials under excess load and rainfall provide an advanced understanding of the landslide process. Landslide characterisation is described through various means, e.g. landslide mechanisms and occurrence force (Leroueil 2001; Take et al. 2004; Huang et al. 2022), failure mode analysis/simulation (Liu et al. 2015; Sidle and Bogaard 2016; Han et al. 2019a), sensitivity/reliability analysis (Rathod and Rao 2012; Nguyen and Likitlersuang 2019; Huang et al. 2020), and the design of effective countermeasure and their field optimisation (Popescu and Sasahara 2009; Han et al. 2019b; Chen et al. 2021). In addition to the physical science investigation, socio-economic analysis of the landslide issues helps to infer the vulnerability of the people living on dangerous slopes and effectively promotes the disaster risk governance (Antronico et al. 2020; Vij et al. 2020; Alam and Ray-Bennett 2021; Huang et al. 2021).

The uplifted south-eastern hilly region of Bangladesh is frequently affected by numerous landslides during the monsoon. Similar hill ranges in north-east India and Myanmar are also landslide prone due to the intense rainfall and uplifted tertiary hill ranges of this region (Singh and Singh 2013; Bhusan et al. 2022). In Bangladesh, landslide-induced fatalities in the Chittagong hill tract are reported yearly. Landslides are now becoming a recurrent natural hazard and are classified as an emergent national threat (Alam 2020; Ahmed 2021; Sultana and Tan 2021). In the last twenty years, landslides caused more than 700 fatalities and more than 1000 injuries. The 2017 landslide event alone caused more than 150 fatalities. Although government and local authorities implemented a significant amount of landslide protection measures, these are insufficient to prevent landslide-induced disasters in the hilly south-eastern region of Bangladesh (Ahmed 2021). As a case study, we assessed the slope stability of shallow landslides occurring in the Kutupalong Rohingya Camp (KRC) area in Bangladesh (Fig. 1). Following the brutal mass killing and genocide in the Rakhine State of Myanmar, over a million Rohingya people fled to Bangladesh in 2017 and took shelter in the KRC area (UNHCR 2019). The KRC comprises elevated terrains, low-rounded hills, and valleys. This refugee settlement causes razes of the forest, hill cutting, and excess load on the hill slope, which results in numerous shallow landslides in the monsoon (June–September) and damage to property and lives. For the humanitarian crisis-affected population to cope with such natural disasters is troublesome work. It

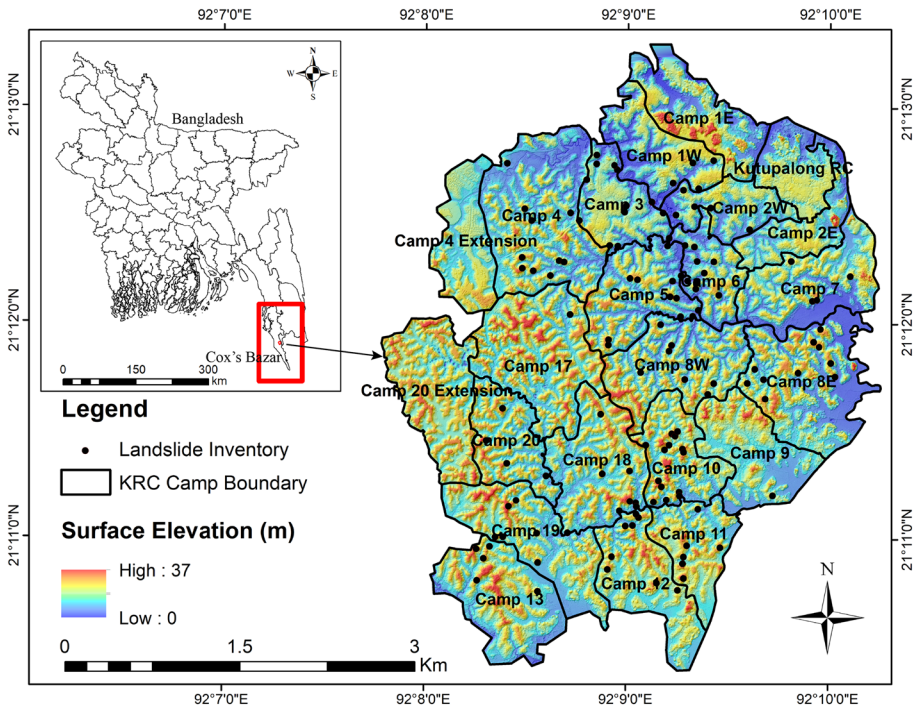


Fig. 1 Location map of the Kutupalong Rohingya camp (KRC) area

worsens during the monsoon season as they live in the temporary makeshift camp and the fragile conditions of the shelters (Alam et al. 2020). Without systematic and effective landslide countermeasures, the resident of the KRC area cannot protect their lives and infrastructure from landslide disasters. A detailed slope failure process, extent, and stability analysis is an inevitable task to design and optimise countermeasures effectively (Sultana and Tan 2021).

The entire KRC area has been affected by hundreds of landslides from 2017 to the present (Figs. 1 and 2). To characterise them for overall slope stability and reliability analysis, average values of the shear strength parameters and four dominant and representative slope angles (40°, 45°, 50°, and 55°), where most landslides occurred, were considered. The area is also composed of almost monotonous lithology and structural setup. Three different slope stability analysis methods were used: geographic information system (GIS)-based infinite slope stability, limit equilibrium method (LEM), and finite element method (FEM). The factor of safety (FoS) determined using these methods was correlated and described the stability state of the slopes. Reliability or sensitivity analysis also assessed uncertainty in the geotechnical properties of the slope materials. The unstable slopes identified from the comparative analysis were further investigated by incorporating the existing landslide mitigation measures. In this way, the performance of the countermeasures to protect the slope was assessed, and the pitfalls of current measures were evaluated (He et al. 2022; Jiang et al. 2022). The results obtained from different slope stability analysis methods can be used in the future to select and implement proper landslide countermeasures in the KRC area.



Fig. 2 Landslides in the Kutupalong Rohingya camp

The perception of the local community on the landslide countermeasures is equally essential to increase their resiliency against landslides. Therefore, a structured and systematic social questionnaire survey was conducted to understand the community response to landslide mitigation measures and their perception. This innovative approach to studying landslide slope stability and its performance and community perception will immensely contribute to DRR strategies.

2 Geological setting and landslide occurrence

The geology of the KRC area is simple and consists of Pliocene to Recent clastic sedimentary deposits (Alam et al. 2003; Kamal et al. 2022b). Tipam sandstone, Girujan clay, and Dupi Tila sandstone formation comprise the entire KRC area (Reimann and Hiller 1993; Hossain et al. 2019). Sandstone and silty shale-type lithology dominate this area. 2 to 5 m residual soil cover is also observed; compositionally, they are identical to the underlying geological units. The camp area has a narrow stream network and rugged geomorphological features of low-rounded hills and valleys. Before the Rohingya settlement, hills were covered with dense vegetation, and valleys were used for agricultural purposes. After the Rohingya settlement, significant land-use changes were observed, and numerous landslide and flash flood events were reported in the KRC area (Ahmed et al. 2020; Alam 2020; Zaman et al. 2020; Hossain and Moniruzzaman 2021; Sakamoto et al. 2021).

Landslide occurs mainly in the residual soil and upper loose, fractured, and partially weathered bedrock of the Pliocene to Pleistocene geological formations (Kamal et al. 2022b). Geological observation of the existing landslide site demonstrates that slide and slump-type slope failures are dominant (Fig. 3). Semicircular sliding plane and well-developed multiple landslide heads were observed where the upper soil has a greater thickness. Otherwise, complex slide and flow-type failure mode is prominent. The landslides in this area are primarily observed in the steep slopes ($> 40^\circ$ slope angle) of natural and anthropogenic reworked origin.

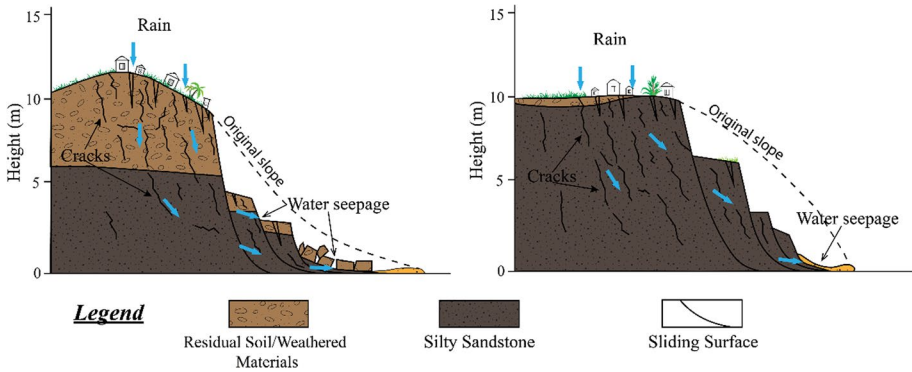


Fig. 3 Schematic geological section of landslides occurring in the KRC area (Kamal et al. 2022b)

Field geological investigation shows a small amount of pore water in the residual soil during the dry period. Still, it increases after the rainfall, and no groundwater influence on landslides was also noticed, as the groundwater table is below the landslide depth in the KRC area. The primary cause of landslides in this area identified through geological fieldwork was low material strength, heavy rain, infiltration due to forest cover removal during the monsoon, and anthropogenic overburden load on the slope.

3 Methodology

This study adopted a cross-disciplinary approach for characterising landslide disaster risk from extensive slope failure. The cause and mechanism of the landslide were evaluated by comparative slope stability analysis using three widely used methods. From this analysis, the stable and unstable slopes were identified. The parameters necessary for slope stability analysis were collected through rigorous fieldwork in the study area. The sensitivity or reliability of the stability analysis was also evaluated using probabilistic computation. The performance of the existing landslide mitigation measures was also assessed using the probabilistic slope stability methods. A social questionnaire survey of $n=404$ respondents was also conducted to evaluate the community’s perception of landslide risk and the effectiveness of the implemented slope failure countermeasures. A brief description of the adopted methods is summarised in the next section.

3.1 Spatial (deterministic) slope stability method

The simple infinite slope stability model is used to determine the spatial distribution of the factor of safety (FoS) in the KRC area. The FoS value is defined concerning the shear strength of the slope soil mass as in Eq. (1),

$$\text{FoS} = \frac{\tau_f}{\tau_d} \tag{1}$$

where τ_f is the shear strength based on the Mohr–Coulomb failure criterion, and τ_d is the shear stress acting in the tangential direction of the slip surface due to the gravity load of the soil mass. A schematic illustration of the infinite slope is shown in Fig. 4.

The shear and normal stress acting on the slip surface of the infinite slope (Fig. 4) is constant and is expressed as:

$$\begin{aligned} \tau &= \gamma z \cos \alpha \sin \alpha, \\ \sigma &= \gamma z \cos^2 \alpha \end{aligned}$$

In the present study area, the water table is far below the slip surface; therefore, the impact of the pore pressure on the landslide is ignored. The statement also justifies that before the Rohingya settlement in this area, no landslide or relict of the landslide was documented. After the Rohingya settlement, a large overburden load facilitates slope failure. After ignoring pore pressure, the equation for FoS calculation can be written as:

$$\text{FoS} = \frac{c' + \gamma z \cos^2 \alpha \tan \varphi'}{\gamma z \cos \alpha \sin \alpha} \tag{2}$$

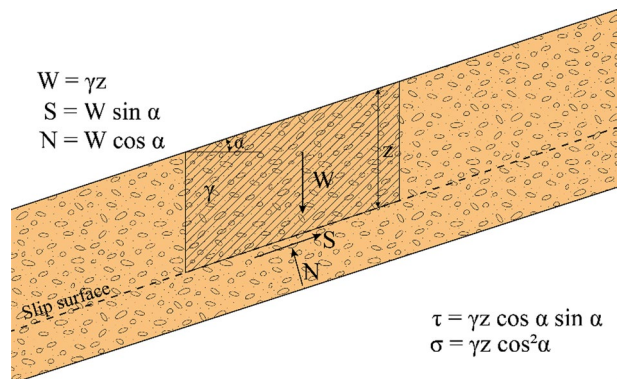
The sliding depth of the landslides in the KRC area is calculated by spatial interpolation of all the sliding depths collected during the landslide inventory survey. This method is implemented in the GIS environment by inputting different raster layers created by interpolating geotechnical field and laboratory measurements (density, cohesion, sliding depth, friction angle, etc.) and surface slope raster created from elevation model in $0.5 \text{ m} \times 0.5 \text{ m}$ raster grid. The computed FoS values for each raster cell by Eq. (2) were classified as unstable, critically stable, and stable according to their FoS value of < 1 , $1\text{--}1.5$, and > 1.5 , respectively.

3.2 Limit equilibrium method (LEM)

The factor of safety (FoS) for the limit equilibrium method (LEM) was determined by Spencer’s method (Spencer 1967). It satisfies both the moment and force equilibrium and considers parallel interslice forces. In Spencer’s method, the interslice forces (Fig. 5) are substituted by an equivalent resultant force Q inclined by a constant angle of θ .

The two-force equilibrium for parallel and perpendicular slices is expressed by:

Fig. 4 Infinite slope model for the spatial factor of safety determination



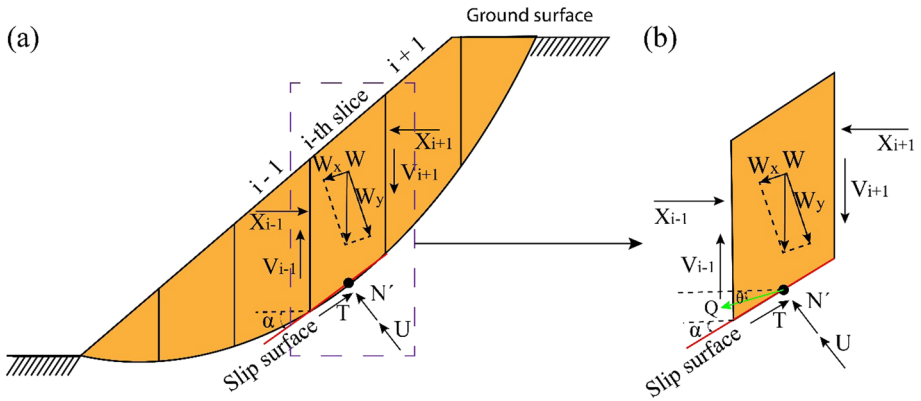


Fig. 5 The 2D stability analysis using Spencer's limit equilibrium method. **a** Forces act on a single slice of a slope, **b** Spencer's method assumption in which interslice forces X_{i-1} , X_{i+1} , V_{i-1} , V_{i+1} are replaced by a single force Q acting at the midpoint of the slice's base

$$\begin{aligned} \Sigma F_x &= 0, \\ T_i - Q_i \cos(a_i - \theta) - W_i \sin a_i &= 0 \end{aligned} \tag{3}$$

and $\Sigma F_y = 0$,

$$N'_i + U_i + Q \sin(a_i - \theta) - W_i \cos a_i = 0 \tag{4}$$

The Mohr–Coulomb criterion is regarding the shear strength of the ground,

$$T_{ULT} = c_i \times L_i + N'_i \tan \varphi_i \tag{5}$$

where T_{ULT} is the shear strength of the soil mass, and L is the length of the slice's base. The shear force T acting on the slice base is,

$$FoS = \frac{T_{ULT}}{T_i} \tag{6}$$

From Eqs. (3) and (6),

$$Q_i = \frac{\frac{c_i \times L_i + W_i \cos a_i - U_i}{FoS} - W_i \sin a_i}{\left(1 + \frac{\tan \varphi_i \times \tan(a_i - \theta)}{FoS}\right) \times \cos(a - \theta)} \tag{7}$$

If the overall moment for the centre of the rotation is zero, then the moment of the internal interslice force Q must be zero,

$$\Sigma Q_i \times R_i \times \cos(a_i - \theta) = 0 \tag{8}$$

where R_i is the distance from the centre of the rotation to the midpoint of each slice.

Therefore, the sum of the internal forces of the entire sliding mass in the vertical and horizontal directions must be zero

$$\Sigma Q_i \times \cos \theta = 0 \tag{9}$$

$$\Sigma Q_i \times \sin \theta = 0 \quad (10)$$

However, since the inclination of the equivalent interslice force Q is constant, Eqs. (9) and (10) are mathematically identical, and both yield

$$\Sigma Q_i = 0 \quad (11)$$

Solving Eqs. (8) and (11) results in two FoS values for a given failure surface, assuming a value of interslice force inclination θ . However, a single value of θ satisfies both moment and force equilibrium. Hence, an iterative procedure to derive this value and the corresponding FoS is applied using the 'Rocscience Slide' software.

3.3 Finite element method (FEM)

The finite element slope stability analysis method uses the shear strength reduction of the critical geotechnical parameters (c' and φ') to calculate the factor of safety (FoS) (Griffiths and Lane 2001). The finite element method (FEM) is frequently used for slope stability analysis alone or in addition to LEM and other methods (Duncan 1996). In this method, the slope materials' original shear strength parameters (c' and φ') are reduced by dividing them with a factor called the strength reduction factor (SRF). As the SRF increases, the slope material strength gradually decreases until the slope reaches the state of equilibrium. The value of SRF at the equilibrium state is considered the factor of safety (FoS) of the slope. The reduced shear strength parameters c'_r and φ'_r are expressed as follows:

$$c'_r = \frac{c'}{\text{SRF}},$$

and

$$\varphi'_r = \tan^{-1} \left(\frac{\tan \varphi'}{\text{SRF}} \right)$$

It should be noted that the SRF is represented as the incremental multiplier (ΣM_{sf}) in Plaxis 2D. When the value of ΣM_{sf} obtained during the analysis is generally constant for several successive steps, then an equilibrium state has been considered fully attained. The shear strength parameters used for FoS simulation and reliability analysis are shown in Table 1.

3.4 Reliability analysis

The factor of safety (FoS) value used to determine the stability state of any particular slope should be commensurate with the uncertainties related to its calculation and

Table 1 Mean shear strength parameters and standard deviation values were used for the LEM and FEM stability and reliability analysis

| Lithology | Unit weight (kN/m ³) | Cohesion (kPa) | Internal friction angle (deg.) |
|------------|----------------------------------|----------------|--------------------------------|
| Upper soil | 17.3 ± 0.34 | 10.67 ± 2.15 | 33.23 ± 1.97 |
| Sandstone | 16.38 ± 0.69 | 6.32 ± 1.85 | 37.6 ± 1.93 |

the consequences of failure (Duncan and Wright 2005). The uncertainties associated with the geotechnical properties of the slope materials are the most crucial factor that prompted several authors to use the reliability and probability of failure (PF) (Kamien 1997; Babu and Mukesh 2015). The probability of failure is determined under specified design conditions when a slope is unstable or $FoS < 1$. For the PF calculation, the distribution of values of the shear strength properties was determined by the 3σ rule described by Dai and Wang (1992).

However, in recent years, it has been realised that the safety factor alone is not a sufficient measure for risk assessment. It is difficult to evaluate how much safer a structure becomes as the factor of safety increases (Duncan 2000; Whitman 2000).

Usually, the appropriate value of the allowable value of the safety factor is based on experience and engineering judgement. Conceptually, geotechnical structures with an aspect of safety of more than 1.0 should be stable. Still, in practice, the acceptable value of the safety factor is significantly greater than unity due to uncertainties related to material variability, measurement and model transformation uncertainty (Phoon and Kulhawy 1999).

Their correlation with FoS values determined the impact and contribution of different shear strength properties on slope stability. Different slope stability analysis scenarios were developed using the dominant slope failure angles observed during the fieldwork. 40° , 45° , 50° , and 55° slope angles are dominant in the KRC to landslide, and different magnitudes of overburden loads (0, 50, and 100 kN/m^2) are assumed. The probabilistic analysis was accomplished through the limit equilibrium method and was implemented in Slide software. From the variation of probability of failure and FoS value, slope failure's consequences are also discussed.

3.5 Evaluation of landslide mitigation measures

To protect the critical settlement and makeshift temporary shelters against landslides or slope failures, different mitigation measures were implemented in the Kutupalong Rohingya Camp (KRC). The essential measures of mitigation observed during the fieldwork in March 2022 were the reinforced terrace (benching) slope, concrete retaining wall, reinforced concrete block structure, slope covering by geo/sandbag, and nature-based slope stabilisation using tree plantation (Fig. 6). Immediate measures to prevent rainfall infiltration slope covering with polythene were also implemented in some vulnerable slopes. During fieldwork, it was found that the landslide mitigation measures successfully protected against slope failure. But in the various location, it was observed that the slope failed, although mitigation measures were present. A performance evaluation of the existing landslide mitigation measures was done to investigate the actual cause and pitfall of the slope stabilisation measures. The performance evaluation of the mitigation measures was carried out by the limit equilibrium method. The necessary data, such as retaining wall strength, slope terrace geometry, and geobag strength, were collected during the fieldwork (Supplementary Table S1). The strength of the concrete retaining structures was measured by the Schmidt hammer rebound process, and the geobag strength was measured by laboratory investigation of the filling sand materials.



Fig. 6 Different landslide mitigation measures implemented in the KRC area

3.6 Social survey procedure

The statistics of the previous landslides and affected households in the KRC area were analysed to describe the landslide disaster risk (IOM 2021; Kamal et al. 2022a). The data on the community's perception of landslide risk, resiliency, and mitigation measures' performance were collected using a structured questionnaire. A total of $n=404$ respondents were questioned from 19–24 March to respond in different formats (see Appendix A): close questions (yes/no), multiple choice questions (5 options), and open-ended questions. The second author led the fieldwork activities in the KRC with the help of six trained field assistants. Before conducting the survey, all the necessary institutional ethical approvals, permission to enter the camp and conduct surveys, and consent from the refugee leaders and respondents were taken. The survey team was trained beforehand, completed risk assessments, and conducted the survey in the Rohingya language. The dataset collected was analysed using SPSS software, and descriptive statistics were used to analyse the responses quantitatively.

4 Results

4.1 Spatial (deterministic) slope stability

The distribution of the factor of safety (FoS) determined by the infinite slope stability method in a spatial grid is shown in Fig. 7. Stability of slopes is classified into three categories based on FoS, e.g. unstable ($FoS < 1$), critically stable ($1 < FoS < 1.5$), and stable

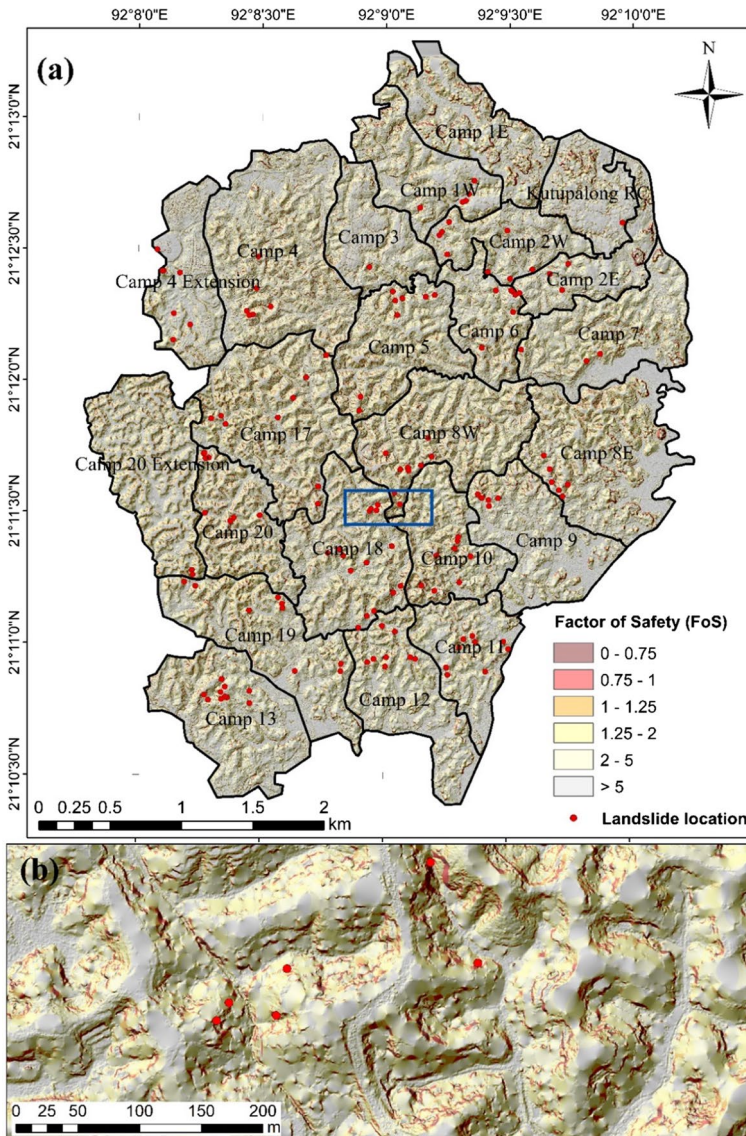


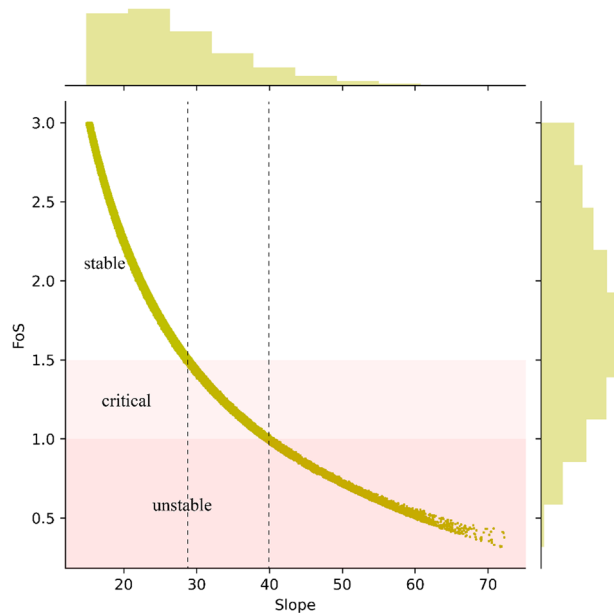
Fig. 7 a Distribution of factor of safety (FoS) calculated using deterministic slope stability (infinite slope) method; b enlarged view

($FoS > 1.5$). The FoS distribution follows the pattern of elevation and slope. It decreases exponentially with slope angle (Fig. 8). Several authors also reported the exponential decrease of FoS with slope angle (Löfroth et al. 2021). The visual inspection of the model result shows that the unstable slopes are concentrated along the steep slopes. Significant slope destabilisation is observed when the slope angle is higher than 40° and critically stable between 28 and 40° (Figs. 7b, 8). In KRC, the abundance of slope angles more elevated than 40° is much smaller, also reflected in the unstable (< 1) FoS value. Although the unstable slope's abundance is less, critically stable slope abundance is much higher in the KRC area. A qualitative comparison of the previous landslide inventory with the produced instability map agrees with the spatial distribution of the FoS values determined using the infinite slope stability framework. Landslide locations were mainly confined within unstable and critically stable areas. The unstable area suggested by the FoS value is frequently concentrated in camps no 4, 5, 8W, 8E, 10, 13, 17, 18, and 20.

4.2 Comparison of LEM and FEM slope stability

Limit equilibrium slope stability is determined for 40° , 45° , 50° , and 55° slope angles, and with overburden loads of 0, 50, and 100 kN/m^2 are illustrated in Fig. 9 and Table 2. The factor of safety (FoS) decreases with increasing slope angle. FoS value of 1.54, 1.37, 1.27, and 1.13 is obtained for 40° , 45° , 50° , and 55° slope angles, respectively, without any overburden load. The slip surface is semicircular and extends from the top of the slope to the base. With increasing slope angle, the base of the slip surface shifted a little distance (Fig. 9) upward. When an overburden load is applied to the ground surface, the FoS value decreases. For 40° and 45° slope angles, the factor of safety value linearly reduces with increasing overburden load but does not attain unstable conditions ($FoS < 1$). But in the case of a 50° slope angle, the unstable condition is reached for 100 kN/m^2 loading, whereas

Fig. 8 Correlation of slope angle and factor of safety (FoS) calculated from the enclosed area of Fig. 7b



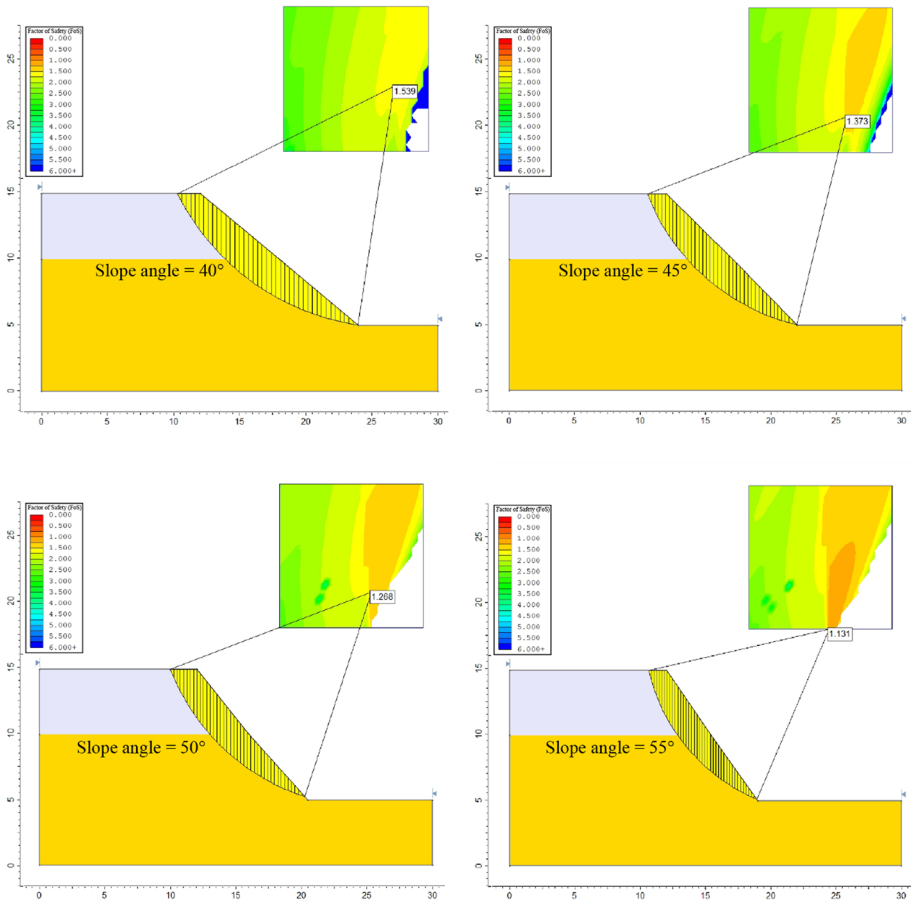


Fig. 9 Safety factor determined for different slope angles under natural conditions without anthropogenic overburden load using the LE method

the unstable condition for a 55° slope is run on both 50 and 100 kN/m² loading. A particular slope angle safety factor value was reduced with increasing load from 0 to 100 kN/m². The radius of the slip surface also decreased (Supplementary Fig. S1). The safety factor (FoS) values determined using LEM are always higher than the FoS values determined using the infinite slope stability method in the GIS grid.

Finite element method (FEM) slope stability is determined for the same stratigraphy, slope angle, and loading as the LEM stability analysis. The factor of safety (FoS) values obtained using FEM are close to the LEM values shown in Table 2.

The distribution of incremental displacement and strain with increasing slope angle is shown in Fig. 10. The FoS value obtained for a 40° slope angle is 1.56 under natural conditions without any stable overburden load. But when an anthropogenic load is applied, the FoS value decreases to 1.28 and 1.12 for 50 and 100 kN/m² loads, respectively. Decreasing trends of FoS with anthropogenic overburden loading occur for all the slope angles and are illustrated for the 45° slope angle in Supplementary Fig. S2. The displacements of slope materials are highest along a narrow semicircular zone which is also attributed to

Table 2 The factor of safety (FoS) is determined for different slope angles and loading

| Slope angle | Loading (kN/m ²) | Factor of safety (FoS) | | Reliability analysis | |
|-------------|------------------------------|------------------------|------|----------------------|-------|
| | | FEM | LEM | PF (%) | RI |
| 40° | 0 | 1.56 | 1.54 | 0 | 5.34 |
| | 50 | 1.28 | 1.34 | 0 | 4.37 |
| | 100 | 1.12 | 1.20 | 0.1 | 2.98 |
| 45° | 0 | 1.44 | 1.37 | 0 | 3.98 |
| | 50 | 1.18 | 1.20 | 0.4 | 2.71 |
| | 100 | 1.05 | 1.06 | 12.9 | 1.13 |
| 50° | 0 | 1.32 | 1.27 | 0.1 | 3.03 |
| | 50 | 1.08 | 1.08 | 11.3 | 1.22 |
| | 100 | 0.95 | 0.98 | 76.2 | -0.73 |
| 55° | 0 | 1.26 | 1.13 | 5.8 | 1.6 |
| | 50 | 0.95 | 0.98 | 64.7 | -0.34 |
| | 100 | 0.83 | 0.87 | 99.2 | -2.48 |

PF probability of failure, *RI* reliability index

maximum strain (Fig. 10). These are possible locations of the slip surface during the slope failures. These slip surface configurations are in good agreement with the LEM-derived slip surfaces.

4.3 Probability of failure and parameter sensitivity

The reliability of slope stability analysis was carried out to determine the probability of failure (PF) and reliability index (RI) of the particular slope, as shown in Fig. 11 and Supplementary Fig. S3. The distribution of field shear strength parameters (c' , ϕ' , γ) has normal distributions. The factor of safety (FoS) value distribution with variable shear strength parameters also showed normal distribution (Fig. 11). With increasing slope angle, the FoS distribution graph approached the left. The probability of failure (PF) is the area delineated by FoS = 1 line and FoS distribution graph; here, it is indicated by the red shaded area (Fig. 11).

The PF value is null for all slope angles in the case of zero anthropogenic overburden load except 55°, which has a 5.82% failure possibility. Failure probability increases with anthropogenic overburden load. For 100 kN/m² overburden load, >75% PF value is obtained for 50° and 55° slopes. Their FoS are also less than 1; i.e. they are always unstable and susceptible to failure. The reliability index (RI) for each of the cases analysed is also shown in Table 2. It shows that all slopes have positive RI except three with less than 1 FoS value. An RI value of more than three is considered entirely safe for work, and here the majority of positive values are more than three or close to 3. These slopes are safe without protection measures.

The correlation of FoS values with shear strength parameters (c' , ϕ' , γ) is equally essential to determine which factor impacts the slope stability more. The scatter or convergence plot of the shear strength parameters (c' , ϕ' , γ) with FoS is shown in Fig. 12. A significant positive correlation exists between the upper soil and lower sandstone layers cohesion (c') and FoS, and the correlation coefficients are 0.51 and 0.75, respectively. The lower sandstone layer's internal friction angle (ϕ') also shows a significant positive correlation (0.42).

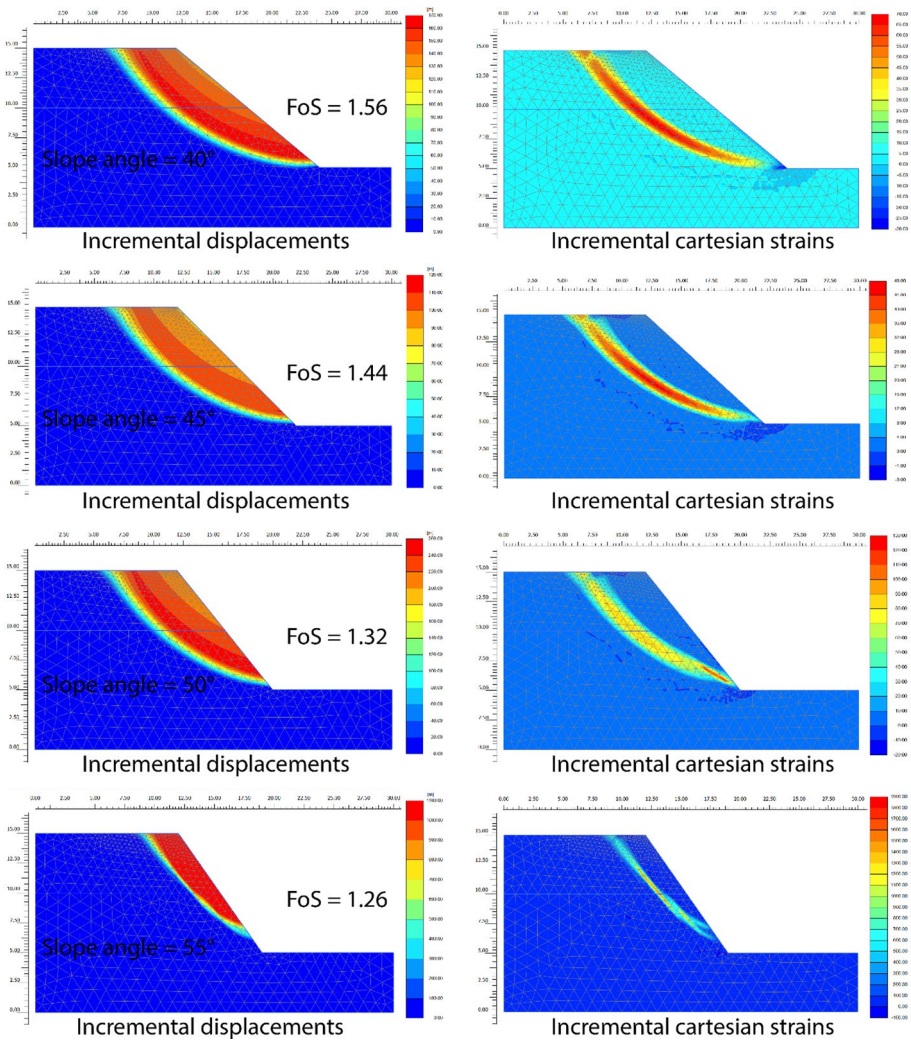


Fig. 10 Safety factor determined for different slope angles under natural conditions without anthropogenic overburden load using the FE method

The unit weight (γ) seems to have no significant correlation. From the analysis of the scatter or convergence plots of the critical shear strength parameters, it is observed that c' and ϕ' of lower sandstone and c' of the upper soil layer are essential components in the stabilisation of slopes.

4.4 Effectiveness of landslide mitigation measures in the KRC area

The comparative slope stability analysis using the limit equilibrium (LEM) and finite element (FEM) modelling shows that slope failure occurs when the slope angle and existing overburden loads from dense shelter construction are significantly high. It is

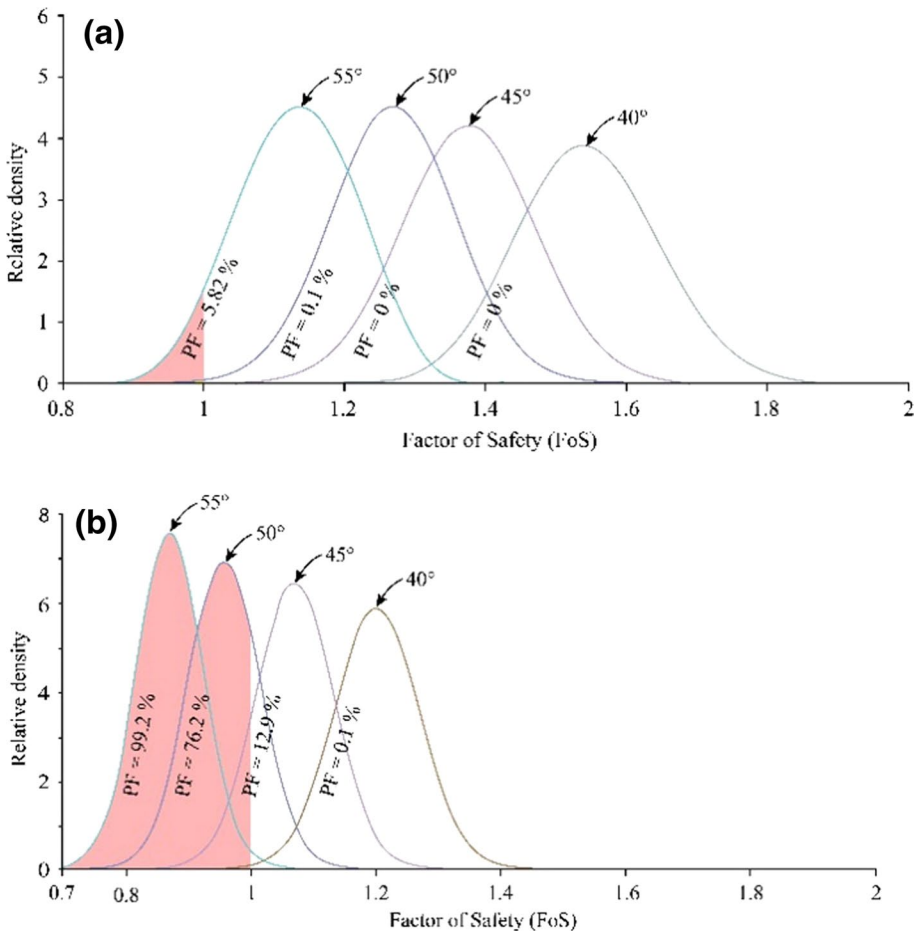


Fig. 11 Results of reliability analysis of slope. **a** Probability of failure (PF) different slope angle under the natural condition without anthropogenic overburden load and **b** with 100 kN/m² overburden load

also observed that among 40°, 45°, 50°, and 55° slope angles and 0, 50, and 100 kN/m² loading, unstable slope conditions exist only for 100 kN/m² loading on 50° slope and both 50 and 100 kN/m² loading on 55° slope. These unstable slopes are protected with different slope stabilisation measures in various locations in the KRC area (Fig. 6). The concrete retaining wall performs significantly well by protecting slope failures for all conditions. It also brought the radius of the slip circle much smaller than the other mitigation measures (Fig. 13a). But for higher loading (≥ 100 kN/m²), some probability of failure also exists for the present retaining wall design parameters, which is evident that a retaining wall protected slope failed after torrential rainfall in camp 15 cause some fatalities in 2021.

The terracing of the slopes with the reinforced bamboo wall increases the factor of safety to a safe limit for 50° and 55° slopes with 100 and 50 kN/m² loading, respectively. Also, the failure probability is significantly low, and the reliability index is close to 3 (Table 2). But for the 55° slope with ≥ 100 kN/m² loading, the slope remains unstable with

the bamboo wall reinforced terracing landslide mitigation measures (Fig. 13b). Hence, landslides in the terrace-protected slopes are occurring and seen in various places in the KRC area.

Implementing slope covering with geo/sandbag (Fig. 14b) protects the slope marginally ($FoS \approx 1$) with a fair share of failure probability for the high slope and loading. For the geo/sandbag-type mitigation measures, it was observed during the fieldwork that the failure of the mitigation measure (geo/sandbag cover) itself causes disaster and fatalities. For example, a 20-year-old woman died in camp 21 (Chakmarkul) in 2021.

4.5 Landslide disaster risk and perception of mitigation measures

This section focuses on the landslide disaster risk based on the observations from fieldwork and analysis of landslide statistics in the KRC area. Also, the local community’s perceptions of the landslide mitigation measures are discussed through survey data analysis and descriptive statistics. Due to improper and unplanned construction of landslide mitigation measures, many of the landslide mitigation measures failed to give protection against landslides in the KRC area, as shown in Table 3 and Fig. 14. In some locations, the failure of the landslide countermeasures itself caused fatalities, but the actual slope remains intact. Nevertheless, apart from some failures, landslide countermeasures substantially reduced the number of landslide occurrences and affected households in the KRC area from 2018 to 2021 (Fig. 15). In 2018, 422 individual landslides caused damage to over 4000 households, which was reduced to 260 landslides and 1200 affected households in 2021.

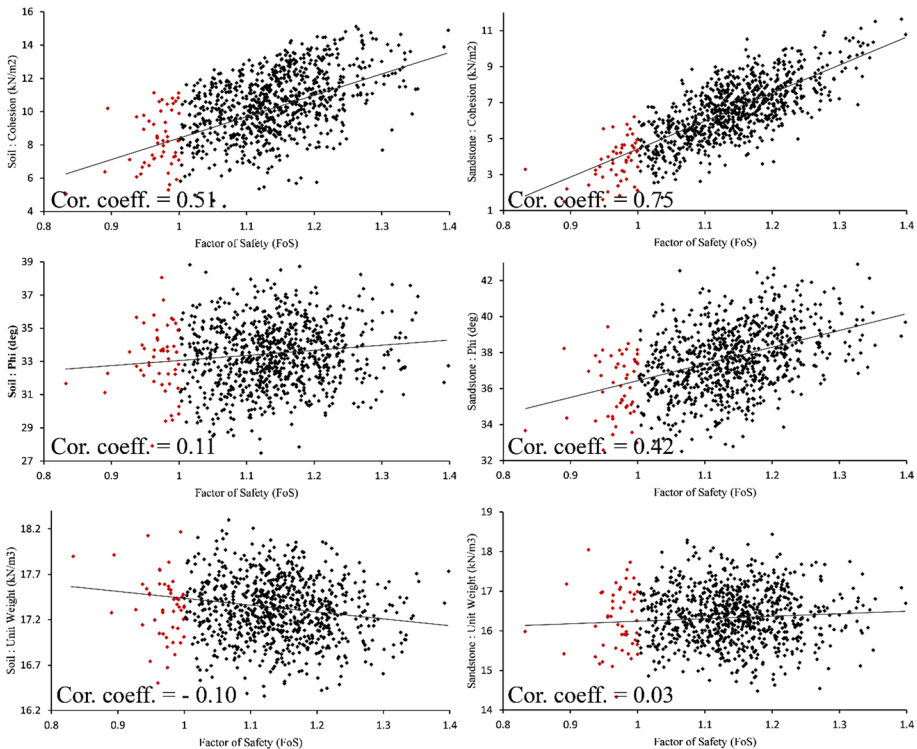


Fig. 12 Correlation between FoS and material properties for 55° slope angle and without loading

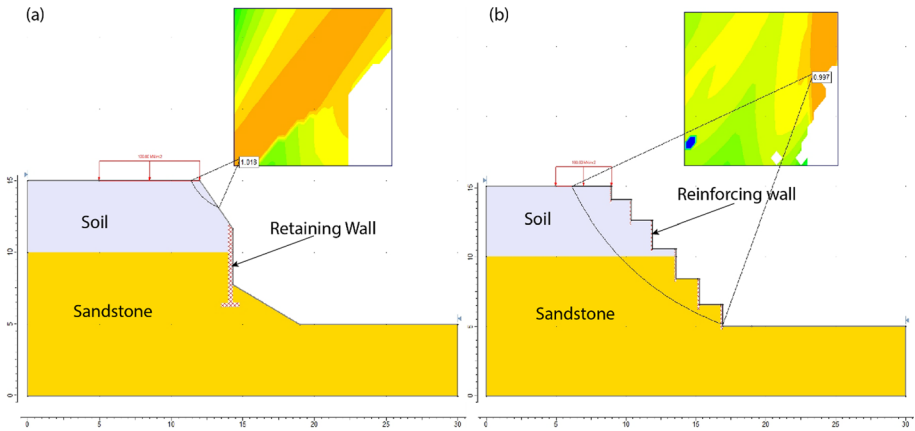
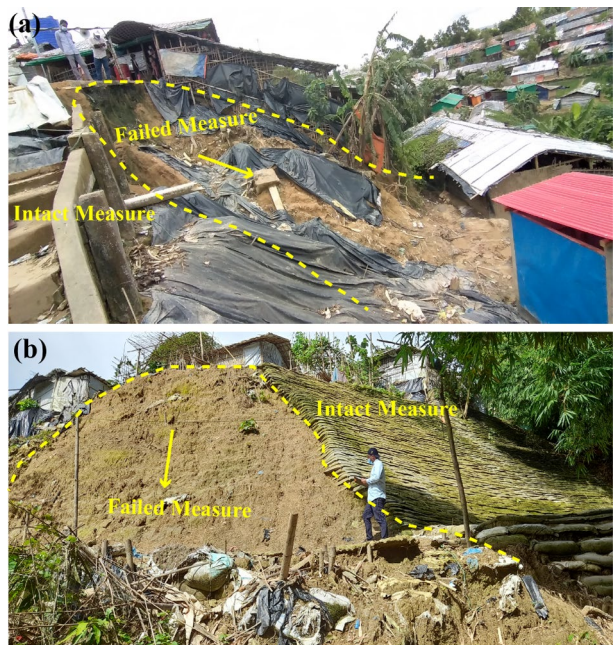


Fig. 13 Safety factor determined for slopes protected against landslide by **a** concrete retaining wall and **b** terrace with the reinforced bamboo wall

Fig. 14 Examples of landslide mitigation measure failure in the Kutupalong Rohingya camp—**a** retaining wall failure and **b** geo/sandbag cover failure

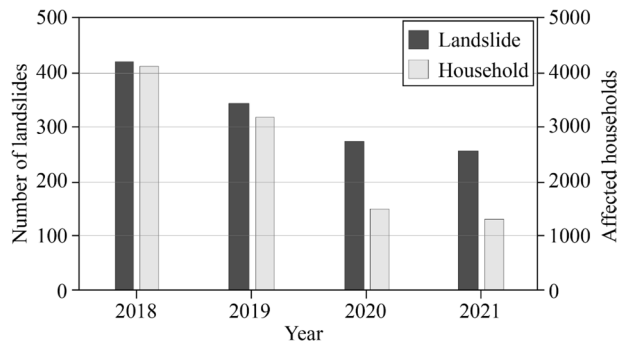


In the questionnaire survey, $n=404$ respondents were asked about various aspects of the impacts of landslides, mainly regarding their mitigation measures. The questions were multiple, primarily choice, and categorical (Appendix A). The responses are graphically shown in Figs. 16 and 17. Among the 404 adult respondents, 57% were male, and 43% were female. They all migrated to the KRC due to humanitarian crises in Myanmar's Rakhine State. About 71% of the surveyed respondents were aged between 20 and 40 years, 24% between 41 and 60 years, and 8% were over 60 years of age (Fig. 16a). Landslides, flash

Table 3 The factor of safety (FoS) for different slope angles and loading after implementing landslide mitigation measures

| Mitigation measure type | Slope angle | Loading (kN/m ²) | Factor of safety (FoS) | | Reliability analysis | |
|--------------------------|-------------|------------------------------|------------------------|-------|----------------------|------|
| | | | Before | After | PF (%) | RI |
| Reinforced terrace slope | 50° | 100 | 0.98 | 1.129 | 0.80 | 2.40 |
| | 55° | 50 | 0.98 | 1.122 | 2.20 | 1.97 |
| Concrete retaining wall | 50° | 100 | 0.87 | 0.997 | 49.1 | 0.01 |
| | | 100 | 0.98 | 1.102 | 16.5 | 0.98 |
| | | 50 | 0.98 | 1.355 | 1.10 | 2.34 |
| Geo/sandbag cover | 50° | 100 | 0.87 | 1.018 | 41.2 | 0.23 |
| | | 100 | 0.98 | 1.065 | 9.20 | 1.34 |
| | | 50 | 0.98 | 1.153 | 0.20 | 2.87 |
| | 55° | 100 | 0.87 | 1.014 | 36.6 | 0.36 |

Fig. 15 Landslide occurrence and affected households in the Kutupalong Rohingya Camp (KRC) from 2018 to 2021. (Data source: IOM 2021)



floods, cyclones/windstorms, and fire hazards were identified to be frequently occurring in the camp areas. Among these hazards, 41% and 30% of respondents had low and high exposure to landslides, respectively, whereas 25% and 4% were not aware of landslides, respectively. The highest number of respondents confronted cyclones/windstorms.

Respondents strongly agreed (80%) that mitigation measures can prevent landslides (Fig. 17); however, a majority of them were doubtful about the effectiveness of the existing mitigation measures (e.g. 23% and 43% ‘strongly disagree’ and ‘disagree’, respectively). About 59% negatively responded to the question, ‘What do you think about the perfection of the mitigation measure construction work?’, whereas 29% were positive, and 11% remained neutral. In response to whether (unsafe and unplanned) mitigation measures contribute to more disasters, approx. 52% of the respondents were neutral or did not think about it; none strongly agreed; 13% agreed with this question; and 32% and 3% disagreed and strongly disagreed, respectively (Fig. 17).

Respondents were also asked which mitigation measures could prevent slope failure in the KRC area. About 70% answered that a concrete retaining wall could be better performed to reduce landslide risk. However, many also suggested that modifying the existing slope by decreasing the slope inclination and planting trees could be a better landslide prevention technique with minimal environmental disturbance.

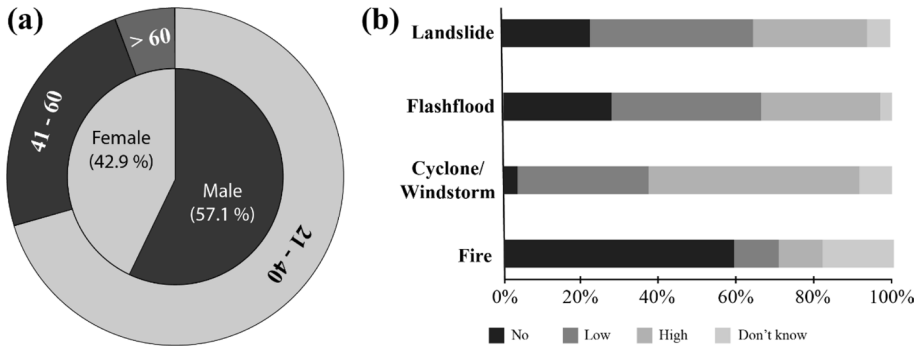


Fig. 16 **a** Basic characteristics (gender: inner circle, and age group: outer circle) and **b** different levels of hazard exposures of the respondents

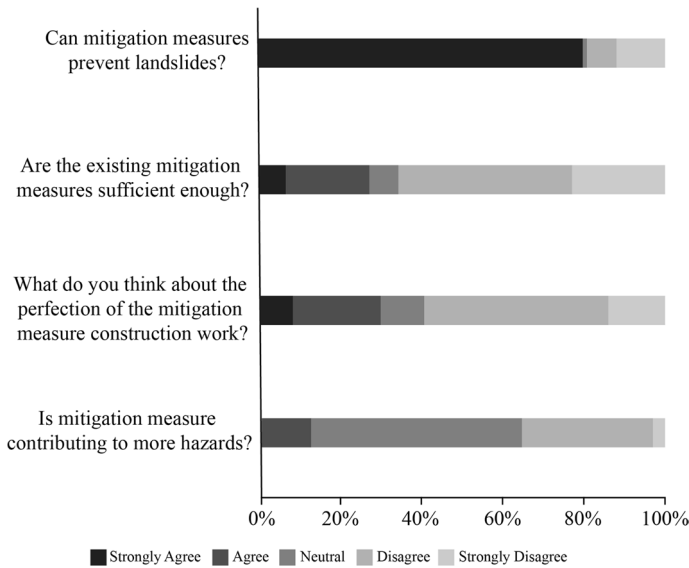


Fig. 17 Respondents answer the questions on the performance of the landslide mitigation measures

5 Discussion and conclusion

The physiography and geological characteristics of the landslides in the KRC area, as observed during the fieldwork, suggest that most of them are rotational slide-type failures and have two stratigraphic layers: upper residual soil and lower sandy formation. Different methods for slope stability analysis give different types of results (Cheng and Lau 2014; Khan and Wang 2020). The factor of safety (FoS) obtained from spatial (infinite slope geometry) stability analysis is much less than that obtained from point-wise analysis using LEM (Spencer’s) and FEM methods. The distribution of FoS obtained from the spatial (infinite) analysis shows an exponentially decreasing trend of FoS with varying slope angles. Similar results are also accepted on the fibrous sediments

by Löfroth et al. (2021) on the Baltic coast of Sweden. The spatial distribution of landslides locations collected from the field is also in good agreement with the results obtained using spatial (infinite) analysis (Fig. 7b). If the state of equilibrium ($FoS = 1$) is set to 1.25 or 1.5, the agreement of the spatial (infinite) analysis results has better accuracy (Dolojan et al. 2021). The slopes with more than 40° inclinations are unstable in the KRC area.

The safety factors determined using LEM and FEM are identical. Both methods have slope failure along a semicircular slip surface. The LEM and FEM consistently demonstrate results close to each other if the structure or stratigraphy has a simple geometry (Rathod and Rao 2012; Ozbay and Cabalar 2015). From LEM and FEM analysis, only three conditions were unstable. However, the effectiveness analysis of these slopes with different mitigation measures shows that landslide countermeasures improve the slope stability only to a marginal level. This demonstrates that unstable slopes were still vulnerable after implementing the countermeasures. This statement was verified in the field that some of the slopes in the KRC area failed in the presence of slope failure protection measures. It was also observed that landslide countermeasures failure caused fatalities, but the slope remains intact. This type of incident is more alarming because the structural countermeasures, in some cases, generate a greater vulnerability (Huang et al. 2021).

The statistical data analysis showed that landslide mitigation measures reduced landslide incidents in the KRC area. The people's perception also reflects that landslide structural countermeasures are functional, but they are more concerned with the type of mitigation measures and their construction quality/reliability. The local community chooses the concrete retaining wall to be the most effective for landslide mitigation which is also evident in other areas (Sultana and Tan 2021). The FoS distribution follows the cohesion and friction angle of lower sandstone, and the cohesion of the upper soil layer is the crucial factor for slope stabilisation. Thus, when designing and implementing any slope protection measures in the KRC area, importance should be given to the lower sandstone layer first and then the upper soil layer. Land-use planning and reorganisation considering the spatial distribution of safety factors will efficiently mitigate and prevent landslide risk.

Three different slope stability analysis approaches were utilised to understand the state of the equilibrium of slopes from the perspective of KRC. In addition, the effectiveness of the mitigation measures was also analysed, and public perception was discussed. The key findings can be summarised as follows:

- The GIS-based spatial (infinite) slope stability analysis method underestimates the safety factor of the slopes compared to the limit equilibrium and finite element methods.
- The LEM- and FEM-derived safety factor values are close to each other. All the slopes are stable or critically stable under natural conditions without anthropogenic interventions. The slip surfaces are semicircular for all the cases of LEM and FEM.
- Significant variations in the probability of failure (PF) were observed, mainly due to the uncertainties in the geotechnical shear strength parameters. The cohesion and friction angle of lower sandstone and the cohesion of upper soil layers are essential in slope stabilisation analysis.
- Although implemented landslide mitigation measures (structural) reduce the number of landslides and affected households, it gives protection to a marginal level having a significant probability of slope failure.
- The local community's preferred countermeasures are flawless and effective construction and structural reliability.

The findings from physical science perspective reveal that various structural measures already undertaken by different NGOs and agencies to mitigate landslide disaster risk in the KRC are mostly unreliable regarding their design safety and dependability concerns. The Rohingyas living on dangerous slopes are also doubtful about the quality of the construction works and their performance during heavy rainfall in protecting their shelters and lives. To achieve the ultimate landslide DRR in the KRC, it is highly recommended to apply other non-structural measures or promote natural-based solutions such as afforestation activities, vetiver grass bioengineering, creating community awareness, operationalising landslide early warning systems, planned relocation to safer places, and fostering repatriation in Myanmar or resettlement in third countries according to the UN mandate.

The proposed method of blending the physical and social science components in understanding and evaluating the landslide structural mitigation measures is innovative and enhances the trustworthiness of the public. Furthermore, the method can be replicated in any landslide context worldwide and advance the knowledge base of landslide disaster risk reduction by generating practical results.

Appendix

Appendix A: Questionnaire used for the social survey

| Landslide risk perception | | Response |
|--|---|--|
| Basic information | | |
| 1 | Gender of the respondent | Male Female Other (specify) |
| 2 | Respondent's age group (years) | 20–40 41–60 > 60 |
| Basic landslide risk perception | | |
| 3 | Do you know what a landslide is? | Yes (Could you briefly describe it?) No |
| 4 | How much do you feel yourself exposed to landslides? | No Low High Do not know/ no idea |
| 5 | How much do you feel yourself exposed to flash floods? | No Low High Do not know/ no idea |
| 6 | How much do you feel yourself exposed to cyclone/windstorm? | No Low High Do not know/ no idea |
| 7 | How much do you feel yourself exposed to fire hazards? | No Low High Do not know/ no idea |
| Landslide mitigation measures | | |

| Landslide risk perception | Response |
|---------------------------|--|
| 8 | What type of mitigation measures are implemented in your reach of slope failure prone areas? Reinforced terrace (benching) slope Concrete retaining wall Reinforced concrete block structure Slope covering by geo/sandbag Nature-based slope stabilisation using tree plantation |
| 9 | Can mitigation measures prevent landslides? Strongly agree Agree Neutral Disagree Strongly disagree |
| 10 | Are the existing mitigation measures sufficient? Strongly agree Agree Neutral Disagree Strongly disagree |
| 11 | What do you think about the perfection of the mitigation measure construction work? Strongly agree Agree Neutral Disagree Strongly disagree |
| 12 | Is mitigation measure contributing to more hazards? Strongly agree Agree Neutral Disagree Strongly disagree |
| 13 | Which types of mitigation measures do you think could prevent slope failure hazards? Reinforced terrace (benching) slope Concrete retaining wall Reinforced concrete block structure Slope covering by geo/sandbag Nature-based slope stabilisation using tree plantation Nothing Others (please specify) |

Supplementary Information The online version contains supplementary material available at <https://doi.org/10.1007/s11069-023-05947-6>.

Author contributions The project involved contributions from multiple authors. Professor A. S. M. Maksud Kamal played a role in developing the project concept and designing fieldwork plans and served as the physical science Co-Applicant. Farhad Hossain and Professor Md Zillur Rahman were responsible for material preparation, data collection, and analysis. Farhad Hossain was the initial author of the manuscript, which was subsequently reviewed and edited by all authors. Dr Bayes Ahmed oversaw the fieldwork activities, revised the manuscript, and served as the project manager. Professor Peter Sammonds acted as the Principal Investigator of the project. The final manuscript was reviewed and approved by all authors.

Funding This research was funded by The Royal Society through the project titled ‘Resilient Futures for the Rohingya Refugees’ (Award Reference: CHL\R1\180288) which is supported under the UK Government’s Global Challenges Research Fund (GCRF). The authors express their gratitude to the Office of the Refugee Relief and Repatriation Commissioner (RRRC), Cox’s Bazar, Bangladesh, for granting permission for conducting fieldwork within the Kutupalong Rohingya Camp.

Data availability statement All the data and materials supporting the results and analyses presented in this paper are available upon request.

Declarations

Competing interests The authors declare no known conflicts of interest that could have appeared to influence the work reported in this paper.

Open Access This article is licensed under a Creative Commons Attribution 4.0 International License, which permits use, sharing, adaptation, distribution and reproduction in any medium or format, as long as you give appropriate credit to the original author(s) and the source, provide a link to the Creative Commons licence, and indicate if changes were made. The images or other third party material in this article are included in the article's Creative Commons licence, unless indicated otherwise in a credit line to the material. If material is not included in the article's Creative Commons licence and your intended use is not permitted by statutory regulation or exceeds the permitted use, you will need to obtain permission directly from the copyright holder. To view a copy of this licence, visit <http://creativecommons.org/licenses/by/4.0/>.

References


- Ahmed B (2021) The root causes of landslide vulnerability in Bangladesh. *Landslides* 1–14. <https://doi.org/10.1007/s10346-020-01606-0>
- Ahmed B, Rahman MS, Sammonds P et al (2020) Application of geospatial technologies in developing a dynamic landslide early warning system in a humanitarian context: the Rohingya refugee crisis in Cox's Bazar, Bangladesh. *Geomatics Nat Hazards Risk* 11:446–468. <https://doi.org/10.1080/19475705.2020.1730988>
- Alam A, Sammonds P, Ahmed B (2020) Cyclone risk assessment of the Cox's Bazar district and Rohingya refugee camps in southeast Bangladesh. *Sci Total Environ* 704:135360. <https://doi.org/10.1016/j.scitotenv.2019.135360>
- Alam E (2020) Landslide hazard knowledge, risk perception and preparedness in southeast Bangladesh. *Sustain* 12:6305. <https://doi.org/10.3390/SU12166305>
- Alam E, Ray-Bennett NS (2021) Disaster risk governance for district-level landslide risk management in Bangladesh. *Int J Disaster Risk Reduct* 59:102220. <https://doi.org/10.1016/j.ijdrr.2021.102220>
- Alam M, Alam MM, Curry JR et al (2003) An overview of the sedimentary geology of the Bengal Basin in relation to the regional tectonic framework and basin-fill history. *Sediment Geol* 155:179–208. [https://doi.org/10.1016/S0037-0738\(02\)00180-X](https://doi.org/10.1016/S0037-0738(02)00180-X)
- Antronico L, De Pascale F, Coscarelli R, Gullà G (2020) Landslide risk perception, social vulnerability and community resilience: the case study of Maierato (Calabria, southern Italy). *Int J Disaster Risk Reduct* 46:101529. <https://doi.org/10.1016/j.ijdrr.2020.101529>
- Babu GLS, Mukesh MD (2015) Effect of soil variability on reliability of soil slopes. *Geotechnique* 54:335–337. <https://doi.org/10.1680/GEOT.2004.54.5.335>
- Bhusan K, Pande T, Kayal JR (2022) Landslide affected areas and challenges imposed in North Eastern Region of India: an appraisal. *Aust J Eng Innov Technol* 4:32–44. <https://doi.org/10.34104/ajeit.022.032044>
- Chen Z, Song D, Dong L (2021) Characteristics and emergency mitigation of the 2018 Laochang landslide in Tianquan County, Sichuan Province, China. *Sci Rep* 11(11):1–16. <https://doi.org/10.1038/s41598-021-81337-x>
- Cheng YM, Lau CK (2014) Slope stability analysis and stabilization. CRC Press
- Dai S-H, Wang M-O (1992) Reliability analysis in engineering applications. Van Nostrand Reinhold, New York
- Dolojan NLJ, Moriguchi S, Hashimoto M, Terada K (2021) Mapping method of rainfall-induced landslide hazards by infiltration and slope stability analysis. *Landslides* 18:2039–2057. <https://doi.org/10.1007/s10346-020-01617-x>
- Duncan JM (1996) State of the art: limit equilibrium and finite-element analysis of slopes. *J Geotech Eng* 122. [https://doi.org/10.1061/\(ASCE\)0733-9410\(1996\)122:7\(577\)](https://doi.org/10.1061/(ASCE)0733-9410(1996)122:7(577))
- Duncan JM (2000) Factors of safety and reliability in geotechnical engineering. *J Geotech Geoenviron Eng* 126. [https://doi.org/10.1061/\(ASCE\)1090-0241\(2000\)126:4\(307\)](https://doi.org/10.1061/(ASCE)1090-0241(2000)126:4(307))
- Duncan JM, Wright SG (2005) Soil strength and slope stability. Wiley
- Froude MJ, Petley DN (2018) Global fatal landslide occurrence from 2004 to 2016. *Nat Hazards Earth Syst Sci* 18:2161–2181. <https://doi.org/10.5194/NHESS-18-2161-2018>
- Garland GG, Olivier MJ (1993) Predicting landslides from rainfall in a humid, sub-tropical region. *Geomorphology* 8:165–173. [https://doi.org/10.1016/0169-555X\(93\)90035-Z](https://doi.org/10.1016/0169-555X(93)90035-Z)

- Griffiths D, Lane PA (2001) Slope stability analysis by finite elements. *Geotechnique* 51:653–654. <https://doi.org/10.1680/geot.51.7.653.51390>
- Han Z, Su B, Li Y, et al (2019a) Numerical simulation of debris-flow behavior based on the SPH method incorporating the Herschel–Bulkeley–Papanastasiou rheology model. *Eng Geol* 255:26–36. <https://doi.org/10.1016/j.enggeo.2019.04.013>
- Han Z, Su B, Li Y et al (2019b) Comprehensive analysis of landslide stability and related countermeasures: a case study of the Lanmuxi landslide in China. *Sci Rep* 9:12407. <https://doi.org/10.1038/s41598-019-48934-3>
- He J, Zhang L, Fan R et al (2022) Evaluating effectiveness of mitigation measures for large debris flows in Wenchuan, China. *Landslides* 19:913–928. <https://doi.org/10.1007/s10346-021-01809-z>
- Hossain F, Moniruzzaman DM (2021) Environmental change detection through remote sensing technique: A study of Rohingya refugee camp area (Ukhia and Teknaf sub-district), Cox’s Bazar, Bangladesh. *Environ Challenges* 2:100024. <https://doi.org/10.1016/j.envc.2021.100024>
- Hossain MS, Khan MSH, Chowdhury KR, Abdullah R (2019) Synthesis of the tectonic and structural elements of the Bengal Basin and its surroundings. pp 135–218
- Huang H, Huang J, Liu D, He Z (2021) Understanding the public responses to landslide countermeasures in southwest China. *Int J Disaster Risk Reduct* 64:102500. <https://doi.org/10.1016/j.ijdrr.2021.102500>
- Huang L, Zhou T, Zhuang S et al (2022) Failure mechanism of a high-locality colluvial landslide in Wanzhou County, Chongqing, China. *Bull Eng Geol Environ* 81:252. <https://doi.org/10.1007/s10064-022-02758-0>
- Huang M, Sun D, Wang C, Keleta I (2020) Reliability analysis of unsaturated soil slope stability using spatial random field-based Bayesian method. *Landslides* 18:. <https://doi.org/10.1007/s10346-020-01525-0>
- Hungre R, Leroueil S, Picarelli L (2014) The Varnes classification of landslide types, an update. *Landslides* 11:167–194. <https://doi.org/10.1007/s10346-013-0436-y>
- IOM (2021) Incident monitoring: Rohingya refugee camps, Bangladesh. IOM Needs and Population Monitoring (NPM) Team, Cox’s Bazar, Bangladesh. The International Organization for Migration (IOM), Bangladesh Mission. https://npm-iom.shinyapps.io/Incident_Dashboard/_w_c04b7eb8/_w_6395fb00/#about. Accessed 23 Jul 2022
- Jiang J, Zhao Q, Jiang H et al (2022) Stability evaluation of finite soil slope in front of piles in landslide with displacement-based method. *Landslides*. <https://doi.org/10.1007/s10346-022-01924-5>
- Kamal ASMM, Hossain F, Ahmed B, Sammonds P (2022a) Analyzing the 27 July 2021 rainfall-induced catastrophic landslide event in the Kutupalong Rohingya Camp in Cox’s Bazar, Bangladesh. *Geoenviron Disasters* 9:17. <https://doi.org/10.1186/s40677-022-00219-0>
- Kamal ASMM, Hossain F, Rahman MZ, et al (2022b) Geological and soil engineering properties of shallow landslides occurring in the Kutupalong Rohingya Camp in Cox’s Bazar, Bangladesh. *Landslides* 1–14. <https://doi.org/10.1007/S10346-021-01810-6>
- Kamien DJ (1997) Engineering and design: introduction to probability and reliability methods for use in geotechnical engineering. Corps of Engineers Washington DC
- Khan MI, Wang S (2020) Comparative study of slope stability of a highway constructed in hilly area using limit equilibrium and finite element methods. *IOP Conf Ser Earth Environ Sci* 514:022023. <https://doi.org/10.1088/1755-1315/514/2/022023>
- Kjekstad O, Highland L (2009) Economic and social impacts of landslides. *Landslides - Disaster Risk Reduct* 573–587. https://doi.org/10.1007/978-3-540-69970-5_30
- Larsen MC, Torres-Sánchez AJ (1998) The frequency and distribution of recent landslides in three montane tropical regions of Puerto Rico. *Geomorphology* 24:309–331. [https://doi.org/10.1016/S0169-555X\(98\)00023-3](https://doi.org/10.1016/S0169-555X(98)00023-3)
- Leroueil S (2001) Natural slopes and cuts: movement and failure mechanisms. *Geotechnique* 51:197–243. <https://doi.org/10.1680/geot.51.3.197.39365>
- Liu SY, Shao LT, Li HJ (2015) Slope stability analysis using the limit equilibrium method and two finite element methods. *Comput Geotech* 63:291–298. <https://doi.org/10.1016/j.comptgeo.2014.10.008>
- Löfroth H, O’Regan M, Snowball I, et al (2021) Challenges in slope stability assessment of contaminated fibrous sediments along the northern Baltic coast of Sweden. *Eng Geol* 289:106190. <https://doi.org/10.1016/J.ENGEO.2021.106190>
- Nguyen TS, Likitlersuang S (2019) Reliability analysis of unsaturated soil slope stability under infiltration considering hydraulic and shear strength parameters. *Bull Eng Geol Environ* 78:5727–5743. <https://doi.org/10.1007/s10064-019-01513-2>
- Ozbay A, Cabalar AF (2015) FEM and LEM stability analyses of the fatal landslides at Çöllolar open-cast lignite mine in Elbistan, Turkey. *Landslides* 12:155–163. <https://doi.org/10.1007/s10346-014-0537-2>
- Petley D (2012) Global patterns of loss of life from landslides. *Geology* 40:927–930. <https://doi.org/10.1130/G33217.1>
- Phoon FH, Kulhawy K-K (1999) Evaluation of geotechnical property variability. *Can Geo- Tech J*

- Popescu ME, Sasahara K (2009) Engineering Measures for Landslide Disaster Mitigation BT - Landslides – Disaster Risk Reduction. In: Sassa K, Canuti P (eds). Springer, Berlin, pp 609–631
- Rathod GW, Rao KS (2012) Finite element and reliability analyses for slope stability of subsansiri lower hydroelectric project: a case study. *Geotech Geol Eng* 30:233–252. <https://doi.org/10.1007/s10706-011-9465-2>
- Reimann K-U, Hiller K (1993) *Geology of Bangladesh*. Schweizerbart'sche Verlagsbuchhandlung
- Sakamoto M, Ullah SMA, Tani M (2021) Land cover changes after the massive Rohingya Refugee Influx in Bangladesh: neo-classic unsupervised approach. *Remote Sens* 13:5056. <https://doi.org/10.3390/rs13245056>
- Sidle RC, Bogaard TA (2016) Dynamic earth system and ecological controls of rainfall-initiated landslides. *Earth-Sci Rev* 159:275–291. <https://doi.org/10.1016/j.earscirev.2016.05.013>
- Singh CD, Singh J (2013) Landslides caused due to ignorance: case studies from northeast India. *J Geol Soc India* 82:91–94. <https://doi.org/10.1007/s12594-013-0123-6>
- Spencer E (1967) A method of analysis of the stability of embankments assuming parallel inter-slice forces. *Géotechnique* 17:11–26. <https://doi.org/10.1680/GEOT.1967.17.1.11>
- Sultana N, Tan S (2021) Landslide mitigation strategies in southeast Bangladesh: Lessons learned from the institutional responses. *Int J Disaster Risk Reduct* 62:102402. <https://doi.org/10.1016/j.ijdrr.2021.102402>
- Take WA, Bolton MD, Wong PCP, Yeung FJ (2004) Evaluation of landslide triggering mechanisms in model fill slopes. *Landslides* 1:173–184. <https://doi.org/10.1007/s10346-004-0025-1>
- UNHCR (2019) *Global trends 2019: forced displacement in 2019*. <https://www.unhcr.org/globaltrends2019/>. Accessed 22 Jan 2021
- Vij S, Russell C, Clark J, et al (2020) Evolving disaster governance paradigms in Nepal. *Int J Disaster Risk Reduct* 50:101911. <https://doi.org/10.1016/j.ijdrr.2020.101911>
- Whitman RV (2000) Organizing and evaluating uncertainty in geotechnical engineering. *J Geotech Geoenviron Eng* 126:583–593. [https://doi.org/10.1061/\(ASCE\)1090-0241\(2000\)126:7\(583\)](https://doi.org/10.1061/(ASCE)1090-0241(2000)126:7(583))
- Zaman S, Sammonds P, Ahmed B, Rahman T (2020) Disaster risk reduction in conflict contexts: Lessons learned from the lived experiences of Rohingya refugees in Cox's Bazar, Bangladesh. *Int J Disaster Risk Reduct* 50:101694. <https://doi.org/10.1016/j.ijdrr.2020.101694>
- Zhuang J, Peng J, Wang G et al (2018) Distribution and characteristics of landslide in Loess Plateau: a case study in Shaanxi province. *Eng Geol* 236:89–96. <https://doi.org/10.1016/J.ENGGEOL.2017.03.001>

Publisher's Note Springer Nature remains neutral with regard to jurisdictional claims in published maps and institutional affiliations.

Authors and Affiliations

A. S. M. Maksud Kamal¹ · Farhad Hossain² · Bayes Ahmed³  · Md. Zillur Rahman¹ · Peter Sammonds³

✉ Bayes Ahmed
bayes.ahmed@ucl.ac.uk

¹ Department of Disaster Science and Climate Resilience, University of Dhaka, Dhaka 1000, Bangladesh

² Department of Geology, University of Dhaka, Dhaka 1000, Bangladesh

³ Institute for Risk and Disaster Reduction (IRDR), University College London (UCL), Gower Street, London WC1E 6BT, UK